High-order sliding mode for an electropneumatic system: A robust differentiator-controller design

Mohamed Smaoui, Xavier Brun, Daniel Thomasset

INTERNATIONAL JOURNAL OF ROBUST AND NONLINEAR CONTROL
Int. J. Robust Nonlinear Control 2008; **18**:481–501
Published online 30 May 2007 in Wiley InterScience (www.interscience.wiley.com). DOI: 10.1002/rnc.1235

High-order sliding mode for an electropneumatic system: A robust differentiator–controller design

M. Smaoui*,†, X. Brun and D. Thomasset

Laboratoire Ampère-UMR CNRS 5005, Bât Antoine de SAINT-EXUPERY, 25, avenue Jean Capelle, 69621 Villeurbanne Cedex, France

SUMMARY

This paper deals with the robust control problem of a pneumatic actuator subject to parameter uncertainties and load disturbances. The control strategies are based on second- and third-order sliding mode approaches. These controllers require measurements of acceleration for feedback. However, accelerometer is seldom used in practical drive systems, because of the complexity they add to the overall process as they are mounted to the load in displacement. For this, a robust differentiator *via* sliding mode is used to estimate the acceleration. A comparative study between the robust differentiator and a classical one is presented. Implementation results of the proposed sliding mode differentiator–controller design on an experimental set-up are given to illustrate the developments. Copyright © 2007 John Wiley & Sons, Ltd.

Received 25 April 2006; Revised 12 April 2007; Accepted 24 April 2007

KEY WORDS: pneumatic systems; sliding mode control; differentiation; experimental results

1. INTRODUCTION

Pneumatic cylinder systems have the potential to provide high output power to weight and size ratios at a relatively low cost. Adding to their simple structure, easy maintenance and low component cost, pneumatic actuators are one of the most common types of industry actuators [1]. However, the complexity of the electropneumatic systems and the important range of control laws are a real industrial problem where the target is to choose the best control strategy for a given application.

In recent years, research efforts have been directed towards meeting this requirement. Most of them have been in the field of feedback linearization [2, 3]. However, reasonably accurate mathematical models for the pneumatic system are required by the feedback linearization.

*Correspondence to: M. Smaoui, Laboratoire Ampère-UMR CNRS 5005, Bât Antoine de SAINT-EXUPERY, 25, avenue Jean Capelle, 69621 Villeurbanne Cedex, France.
†E-mail: mohamed.smaoui@insa-lyon.fr; URL: http://www-ampere-lyon.fr

A number of investigations have been conducted on fuzzy control algorithms [4], adaptive control [5], backstepping control [6], and robust linear control [7].

Another rather theoretically attractive robust approach is the standard sliding mode control [8]. It is believed that a robust controller can be derived based on rather little information of the system. This approach has been used in several works in order to control pneumatic systems [9–11]. The standard sliding mode features are high accuracy and robustness with respect to various internal and external disturbances. Specific drawback presented by the classical sliding mode techniques is the chattering phenomenon [12]. In order to overcome this drawback, a research activity aimed to find an alternative continuous control guaranteeing the same performances as in classical sliding mode control. The resulting algorithms, turned out to belong to the class of high-order sliding mode (HOSM) control [13].

In [14], a sliding mode controller based on twisting algorithm is designed for an electropneumatic actuator. In [15], a third-order sliding mode controller is designed for the same experimental set-up as [14]. This approach combines standard sliding mode control with linear quadratic one over a finite time interval with a fixed final state.

In the first part of the present paper, two HOSM controllers are designed and tested on an experimental pneumatic actuator set-up. Good performance, robustness against parameter uncertainties, and simple implementation are the main features of the proposed methods. These two feedback controllers require the measurement of acceleration for feedback. However, accelerometers are seldom used in practical drive systems. Indeed, the use of accelerometers adds cost, energy consumption, increases the complexity of the overall system (the accelerometer is mounted to the load in displacement), and reduces its reliability.

Many schemes for the estimation of states variables have been proposed in recent years. Some of these methods are based on nonlinear observer theory such as high gain observer [16], sliding mode observer [12], and backstepping observer [17]. However, nonlinear state observers are difficult to implement when poor knowledge on the system dynamics is available. Therefore, research on modelling and identification is necessary to improve the performance of observers.

For mechanical systems, numerical differentiation method is another attractive method for the estimation of state variables. Indeed, differentiators are very useful tools to determine and estimate signals. For instance, using differentiators, the velocity and acceleration can be computed from the position measurements. However, the design of an ideal differentiator is a difficult and a challenging task. In [18], the author discusses the properties and the limitations of two different structures of linear differentiation systems. A predictive algorithm, which is applied to angular acceleration measurements, is presented in [19]. A robust first-order differentiator *via* HOSM technique is proposed in [20]. The differentiator considered features simple form and easy design and can be employed in real-time control systems.

Following [20], we develop in this paper a robust differentiator *via* sliding mode applied to acceleration measurements. The goal is to show the importance of the choice of the differentiator design in the control of an electropneumatic system.

The paper is organized as follows. The following section describes the model of the electropneumatic actuator. Section 3 deals with the design of a second-order sliding mode controller for this system. Section 4 presents a third-order sliding mode controller. Section 5 presents the robust differentiator *via* second-order sliding mode. Simulation results are presented to compare the robust differentiator to a classical one. Section 6 will be devoted to the experimental results. Both sets of results will be compared according to an industrial benchmark. Section 7 concludes the paper.

DOI: 10.1002/rnc

2. ELECTROPNEUMATIC SYSTEM MODELLING

The considered system (Figure 1) is a linear inline double acting electropneumatic servodrive using a single rod controlled by two three-way servodistributors. The actuator rod is connected to one side of the carriage and drives an inertial load on guiding rails. The total moving mass is 17 kg.

The electropneumatic system model can be obtained using three physical laws: the mass flow rate through a restriction, the pressure behaviour in a chamber with variable volume, and the fundamental mechanical equation.

The pressure evolution law in a chamber with variable volume is obtained assuming the following assumptions [21]: air is a perfect gas and its kinetic energy is negligible; the pressure and the temperature are supposed to be homogeneous in each chamber; and the process is polytropic and characterized by coefficient k. Moreover, the electropneumatic system model is obtained by combining all the previous relations and assuming that the temperature variation is negligible with respect to average and equal to the supply temperature. The dynamics of the servodistributors may be neglected. So, the servodistributors model can be reduced to a static one described by two relationships $q_{m\mathrm{P}}(u, p_{\mathrm{P}})$ and $q_{m\mathrm{P}}(-u, p_{\mathrm{N}})$ between the mass flow rates $q_{m\mathrm{P}}$ and $q_{m\mathrm{N}}$, the input voltages u and the output pressures p_{P} and p_{N}.

The mechanical equation includes pressure force, friction and an external constant force due to atmospheric pressure. So the following equation gives the model of the above system:

$$\begin{aligned}
\frac{\mathrm{d}y}{\mathrm{d}t} &= v \\
\frac{\mathrm{d}v}{\mathrm{d}t} &= \frac{1}{M}[S_{\mathrm{P}}p_{\mathrm{P}} - s_{\mathrm{N}}p_{\mathrm{N}} - bv - F_{\mathrm{ext}}] \\
\frac{\mathrm{d}p_{\mathrm{P}}}{\mathrm{d}t} &= \frac{krT}{V_{\mathrm{P}}(y)}\left[q_{m\mathrm{P}}(u, p_{\mathrm{P}}) - \frac{S_{\mathrm{P}}}{rT}p_{\mathrm{P}}v\right] \\
\frac{\mathrm{d}p_{\mathrm{N}}}{\mathrm{d}t} &= \frac{krT}{V_{\mathrm{N}}(y)}\left[q_{m\mathrm{N}}(-u, p_{\mathrm{N}}) - \frac{S_{\mathrm{N}}}{rT}p_{\mathrm{N}}v\right]
\end{aligned} \tag{1}$$

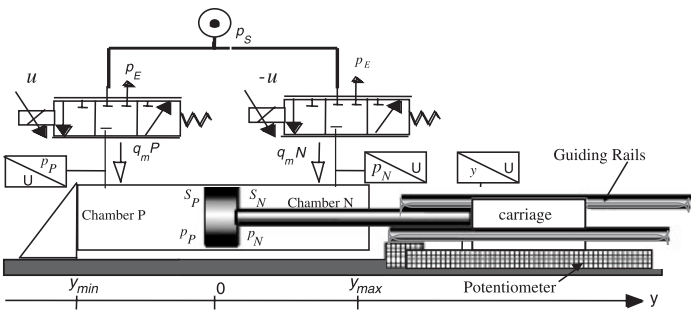

Figure 1. The electropneumatic system.

DOI: 10.1002/rnc

where

$$\begin{aligned} V_{\mathrm{P}}(y) &= V_{\mathrm{P}}(0) + S_{\mathrm{P}} y \\ V_{\mathrm{N}}(y) &= V_{\mathrm{N}}(0) - S_{\mathrm{N}} y \end{aligned} \quad \text{with} \quad \begin{aligned} V_p(0) &= V_{\mathrm{DP}} + S_{\mathrm{P}} \frac{l}{2} \\ V_{\mathrm{N}}(0) &= V_{\mathrm{DN}} + S_{\mathrm{N}} \frac{l}{2} \end{aligned}$$

are the piping volumes of the chambers for the zero position and $V_{\mathrm{D\ (P\ or\ N)}}$ are dead volumes present on each extremities of the cylinder. The main difficulty for model (1) is to know the mass flow rates $q_{m\mathrm{P}}$ and $q_{m\mathrm{N}}$.

In order to establish a mathematical model of the power modulator flow stage, many research works present approximations based on physical laws [22] by modelling of the geometrical variations of the restriction areas of the servodistributor, as well as by experimental characterization [23].

In this paper, the results of the global experimental method giving the static characteristics of the flow stage [24] have been used. The global characterization corresponds to the static measurement of the output mass flow rate q_m, which depends on the input control u and the output pressure p, for constant source and exhaust pressure. The global characterization has the advantage of obtaining simply, by projection of the characteristic series $q_m(u,p)$ on different planes:

- The mass flow rate characteristics series (plane p–q_m).
- The mass flow gain characteristics series (plane u–q_m).
- The pressure gain characteristics series (plane u–p).

The authors in [25] have developed analytical models for both simulation and control purposes. The flow stage characteristics were approximated characteristics by polynomial functions affined in control such that

$$q_m(u,p) = \varphi(p) + \psi(p, \mathrm{sgn}(u))u \tag{2}$$

where $\psi(.) > 0$ over the physical domain. Then, the nonlinear affine model is then given by the following equation:

$$\dot{x} = f(x) + g(x)u \tag{3}$$

where x, $f(x)$ and $g(x)$ in R^4, u in R, and

$$x = (y, v, p_{\mathrm{P}}, p_{\mathrm{N}})^{\mathrm{T}} \tag{4}$$

$$f(x) = \begin{pmatrix} v \\ \dfrac{1}{M}[S_{\mathrm{P}} p_{\mathrm{P}} - S_{\mathrm{N}} p_{\mathrm{N}} - bv - F_{\mathrm{ext}}] \\ \dfrac{krT}{V_{\mathrm{P}}(y)}\left[\varphi(p_{\mathrm{P}}) - \dfrac{S_{\mathrm{P}}}{rT} p_{\mathrm{P}} v\right] \\ \dfrac{krT}{V_{\mathrm{N}}(y)}\left[\varphi(p_{\mathrm{N}}) + \dfrac{S_{\mathrm{N}}}{rT} p_{\mathrm{N}} v\right] \end{pmatrix} \tag{5}$$

DOI: 10.1002/rnc

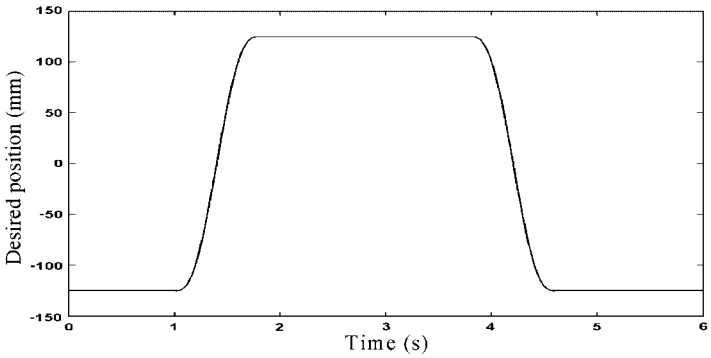

Figure 2. Desired position (mm).

$$g(x) = \begin{pmatrix} 0 \\ 0 \\ \dfrac{krT}{V_{\mathrm{P}}(y)} \cdot \psi(p_{\mathrm{P}}, \mathrm{sgn}(u)) \\ -\dfrac{krT}{V_{\mathrm{N}}(y)} \cdot \psi(p_{\mathrm{N}}, \mathrm{sgn}(-u)) \end{pmatrix} \tag{6}$$

Using (3), the control law is synthesized in the next section.

Two kinds of uncertainties are taken into account: uncertainties due to the identification of physical parameters and uncertainties due to variations of environment. The viscous friction coefficient value has been identified and the variation of this coefficient around the nominal value has been experimentally evaluated at 30%. The mass flow rate delivered by each servodistributor has been approximated by polynomial functions (2). The uncertainties on $\varphi(.)$ and $\psi(.)$ are evaluated to 30 and 15%, respectively. Finally, during the load moving, the total mass in displacement can evolve from 17 kg until 32 kg. The nominal mass is 17 kg.

The aim of the control law is to respect a good accuracy in terms of position tracking for a desired trajectory. The relative degree of the position is three. This means that the electropneumatic system can only track position trajectory at least three times differentiable. The desired trajectory has been carefully chosen in order to respect the differentiability required [26] (see Figure 2).

3. SECOND-ORDER SLIDING MODE CONTROLLER

3.1. Second-order sliding mode

The effective application of sliding mode control to pneumatic systems needs to resolve the problem related to the chattering phenomenon on the switching control signals [12]. Higher-order sliding modes appear to be suitable to counteract these problems [13, 27, 28].

Let $s(x, t)$ be the sliding variable, $s(x, t) \in R$, $x \in R^n$, t is the time. The rth order sliding mode is determined by the equalities $s = s = \dot{s} = \ddot{s} = \cdots = s^{(r-1)} = 0$, which form an r-dimensional

DOI: 10.1002/rnc

condition on the state of the dynamic system. In general, any r-sliding controller needs $s, \dot{s}, \ddot{s}, \ldots, s^{(r-1)}$ to be made available, i.e. 2-sliding controller needs s and $\dot{s}$ to be made available [13].

Consider system (7) with relative degree equal to two with respect to the input:

$$\begin{aligned} \dot{z}_1 &= z_2 \\ \dot{z}_2 &= \phi(x,t) + \Lambda(x,t)u \end{aligned} \tag{7}$$

where $z_1 = s$, $z_2 = \dot{s}$, $u \in R$, and $\phi(x,t)$, $\Lambda(x,t)$ are uncertain functions with $0 < |\phi(x,t)| \leqslant C_0$ and $0 < k_m \leqslant \Lambda(x,t) \leqslant k_{\mathrm{M}}$.

Several 2-sliding algorithms have been presented in the literature [13, 27, 28]. In [14], the well-known twisting algorithm [13] is used in order to design a robust controller for the electropneumatic system. In this paper, the algorithm with a prescribed convergence law is used. In this case, the control law is defined as follows [13, 28]:

$$u = -\alpha \operatorname{sgn}(\dot{s} - g(s)) \tag{8}$$

where $\alpha > 0$, and the continuous function $g(s)$ is smooth everywhere except on $s = 0$. It is assumed that all the solutions of the equation $\dot{s} = g(s)$ vanish in a finite time and the function $(\partial g(s)/\partial s)g(s)$ is bounded:

$$\left| \frac{\partial g(s)}{\partial s} g(s) \right| < C_1 \tag{9}$$

When (8) is used, the trajectories converge first to the equation $\dot{s} = g(s)$ and then to the origin in finite time. The sufficient condition for the finite time convergence to the sliding manifold is defined by the following inequality [28]:

$$\alpha > \frac{C_0 + C_1}{K_m} \tag{10}$$

3.2. Sliding variable and control synthesis

Let us define a sliding surface by

$$s_2 = \lambda(y - y_{\mathrm{d}}) + (\dot{y} - \dot{y}_{\mathrm{d}}) \tag{11}$$

where λ is a positive parameter. Consider the second time derivative of s:

$$\ddot{s}_2 = \alpha(x) + \beta(x)u \tag{12}$$

with

$$\begin{aligned} \alpha(x) = {} & \lambda\left(\frac{1}{M}[S_{\mathrm{P}}p_{\mathrm{P}} - S_{\mathrm{N}}p_{\mathrm{N}} - bv - F_{\mathrm{ext}}] - a_{\mathrm{d}}\right) \\ & + \frac{krT}{M}\left[\frac{S_p}{V_p(y)}\varphi(p_p) - \frac{S_{\mathrm{N}}}{V_{\mathrm{N}}(y)}\varphi(p_{\mathrm{N}}) - \frac{v}{rT}\left(\frac{S_p^2 p_{\mathrm{P}}}{V_{\mathrm{P}}(y)} + \frac{S_{\mathrm{N}}^2 p_{\mathrm{N}}}{V_{\mathrm{N}}(y)}\right)\right] \\ & - \frac{b}{M^2}(S_{\mathrm{P}}p_{\mathrm{P}} - S_{\mathrm{N}}p_{\mathrm{N}} - bv - F_{\mathrm{ext}}) - j_{\mathrm{d}} = \alpha_n(x) + \Delta\alpha(x) \end{aligned} \tag{13}$$

DOI: 10.1002/rnc

and

$$\beta(x) = \frac{S_P}{M}\frac{krT}{V_P(y)}\psi(p_P, \mathrm{sgn}(u)) + \frac{S_N}{M}\frac{krT}{V_N(y)}\psi(p_N, \mathrm{sgn}(-u)) = \beta_n(x) + \Delta\beta(x) \tag{14}$$

Functions $\Delta\alpha(x)$ and $\Delta\beta(x)$ contain all uncertainties, i.e. the leakage polynomial function, friction, and load disturbances. Using the static feedback:[‡]

$$u = \beta_n^{-1}(x)(-\alpha_n(x) + w_2) \tag{15}$$

w_2 is the new control input, one gets:

$$\ddot{s}_2 = \left(\Delta\alpha(x) - \frac{\Delta\beta(x)}{\beta_n(x)}\alpha_n(x)\right) + \left(1 + \frac{\Delta\beta(x)}{\beta_n(x)}\right)w_2 \tag{16}$$

There exist three positive constants C_2, K_m and K_M so that [13]:

$$\left|\left(\Delta\alpha(x) - \frac{\Delta\beta(x)}{\beta_n(x)}\alpha_n(x)\right)\right| < C_2 \tag{17}$$

$$K_m < \left(1 + \frac{\Delta\beta(x)}{\beta_n(x)}\right) < K_M \tag{18}$$

Then, one can apply the second-order algorithm previously presented:

$$w_2 = -\alpha_2\,\mathrm{sgn}(\dot{s}_2 - g(s_2)) \tag{19}$$

The function $g(s_2)$ is chosen as follows [13]:

$$g(s_2) = -k|s_2|^{1/2}\,\mathrm{sgn}(s_2) \tag{20}$$

Finally, a sliding mode occurs on $s_2 = \dot{s}_2 = 0$ leading to desired tracking property for the position. It is important to note that the validity of the position control law depends on the stability of the unobservable subsystem, which is one dimensional. It is very difficult to obtain results about the global stability of the zero dynamics but the local stability has been proved [29].

4. THIRD-ORDER SLIDING MODE CONTROLLER

4.1. Third-order sliding mode

Consider a single input nonlinear system:

$$\begin{aligned} \dot{x} &= f(x) + g(x)u \\ y &= s(x,t) \end{aligned} \tag{21}$$

where $s(x,t) \in R, x \in R^n, t$ is the time. Suppose that the control objective is to force $s(x,t)$ to zero. By differentiating three times the sliding surface s, under the assumption that system (21)

[‡]According to the physical domain, the scalar $\beta_n(x)$ is never equal to 0.

DOI: 10.1002/rnc

has relative degree *versus* s equal to three, it leads that there exists two functions $a(x,t)$ and $b(x,t)$ such that

$$\begin{aligned}\dot{z}_1 &= z_2\\ \dot{z}_2 &= z_3\\ \dot{z}_3 &= a(x,t) + b(x,t)u\end{aligned} \tag{22}$$

where $z_1 = s$, $z_2 = \dot{s}$, $z_3 = \ddot{s}$, $u \in R$ and $a(x,t)$, $b(x,t)$ are uncertain functions with $0 < |a(x,t)| \leqslant C_0$ and $0 < k_m \leqslant b(x,t) \leqslant k_M$.

System (21) satisfies a third-order sliding mode with respect to the sliding variable s if its state trajectories lie on the intersection of the three manifolds $s = 0$, $\dot{s} = 0$, and $\ddot{s} = 0$ in the state space.

4.2. Sliding variable and control synthesis

Let us define the sliding surface by

$$s_3 = (y - y_{\mathrm{d}}) \tag{23}$$

which represent the position error. The relative degree of the position is equal to three. It is easy to check that the control input appears explicitly in the third total time derivative of s. In this case, a first- and second-order sliding mode cannot be used. A third-order sliding mode algorithm appears to be suitable to counteract this problem.

By using (3), the following equations are obtained:

$$\dot{s}_3 = (v - v_{\mathrm{d}}) \tag{24}$$

$$\ddot{s}_3 = (a - a_{\mathrm{d}}) \tag{25}$$

$$\dddot{s}_3 = \chi(x) + (\beta_n(x) + \Delta\beta(x))u \tag{26}$$

$$\begin{aligned}\chi(x) &= \frac{krT}{M}\left[\frac{S_p}{V_p(y)}\varphi(p_p) - \frac{S_{\mathrm{N}}}{V_{\mathrm{N}}(y)}\varphi(p_{\mathrm{N}}) - \frac{v}{rT}\left(\frac{S_p^2 p_{\mathrm{P}}}{V_{\mathrm{P}}(y)} + \frac{S_{\mathrm{N}}^2 p_{\mathrm{N}}}{V_{\mathrm{N}}(y)}\right)\right]\\ &\quad - \frac{b}{M^2}(S_{\mathrm{P}}p_{\mathrm{P}} - S_{\mathrm{N}}p_{\mathrm{N}} - bv - F_{\mathrm{ext}}) - j_{\mathrm{d}}\\ &= \chi_n(x) + \Delta\chi(x)\end{aligned} \tag{27}$$

Using the static feedback:

$$u = \beta_n^{-1}(x)(-\chi_n(x) + w_3) \tag{28}$$

w_3 is the new scalar control input, one gets:

$$\dddot{s}_3 = \left(\Delta\chi(x) - \frac{\Delta\beta(x)}{\beta_n(x)}\chi_n(x)\right) + \left(1 + \frac{\Delta\beta(x)}{\beta_n(x)}\right)w_3 \tag{29}$$

DOI: 10.1002/rnc

A third-order sliding mode controller for an electropneumatic system based on optimal linear quadratic control is presented in [15]. A family of r-sliding mode controllers with finite time convergence for any natural number r is presented in [30]. In this paper, a third-order sliding mode controller from this family is used. In this case, only a single scalar parameter α_3 is to be adjusted. Indeed, the new control input w_3 can be chosen as follows:

$$w_3 = -\alpha_3 \operatorname{sgn}(\ddot{s}_3 + 2(|\dot{s}_3|^3 + |s_3|^2)^{1/6} \operatorname{sgn}(\dot{s}_3 + |s_3|^{2/3} \operatorname{sgn}(s_3))) \tag{30}$$

5. A ROBUST DIFFERENTIATOR *VIA* SECOND-ORDER SLIDING MODE

5.1. The robust differentiator

In general, any 2-sliding controller needs the sliding surface and its derivative to be made available and is determined by the equalities $s = \dot{s} = 0$. The super twisting algorithm does not require the time derivative of the sliding variable [13]. In this section, a robust differentiator *via* sliding mode technique is studied. Indeed, a robust exact differentiation *via* sliding mode technique is proposed in [20]. The differentiator considered features simple form and easy design. It was synthesized to be employed in real-time control systems.

Without loss of generality, let input signal $f(t)$ be a measurable function and let it consists of a base signal having a derivative with Lipschitz's constant $C > 0$. In order to differentiate the input signal, consider the auxiliary equation:

$$\dot{x} = v \tag{31}$$

Consider now the following sliding surface, which represents the difference between x and $f(t)$:

$$s = x - f(t) \tag{32}$$

By differentiating (32), it leads to the following relationship:

$$\dot{s} = v - \dot{f}(t) \tag{33}$$

The super twisting algorithm defines the control law v as

$$v = v_1 - \lambda |s|^{1/2} \operatorname{sgn}(s) \tag{34}$$

with

$$\dot{v}_1 = -w \operatorname{sgn}(s) \tag{35}$$

where $w, \lambda > 0$. Here v is the output of the differentiator. Indeed, the super twisting algorithm converges in finite time, so the following relationship can be obtained in finite time:

$$\dot{x} - \dot{f}(t) = v - \dot{f}(t) = 0 \tag{36}$$

or

$$v = \dot{f}(t) \tag{37}$$

DOI: 10.1002/rnc

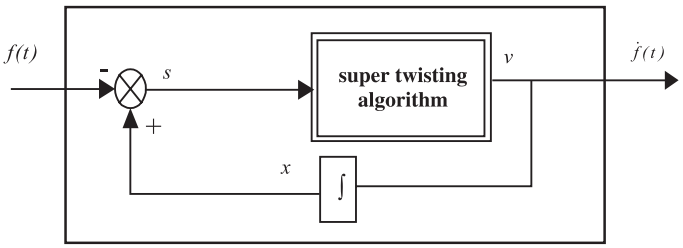

Figure 3. The structure of the differentiator.

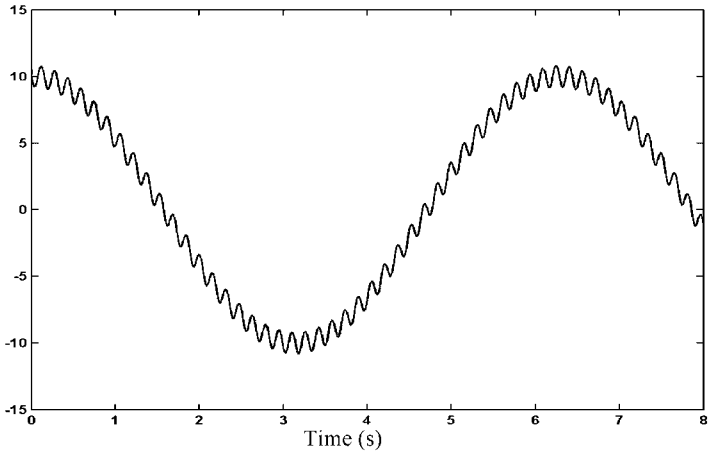

Figure 4. Simulation results.

The corresponding sufficient conditions for finite time convergence are [20]

$$w > C \tag{38}$$

$$\lambda^2 \geqslant 4C\frac{w+C}{w-C} \tag{39}$$

Figure 3 presents the structure of (34). The separation principle is fulfilled for the proposed differentiator. A combined differentiator–controller output feedback preserves the main features of the controller with the full state available [31].

5.2. Simulation results

Firstly, the input signal is chosen as:

$$f(t) = 10\sin(t) + 0.02\cos(40t) \tag{40}$$

Figure 4 presents the output of the differentiator and the ideal derivative of $f(t)$ ($\dot{f}(t) = 10\cos(t) - 0.8\sin(40t)$).

It is noticed that the robust differentiator output (34) and the analytical derivative of the function are identical in a remarkable way. However, the choice of a method of derivation

DOI: 10.1002/rnc

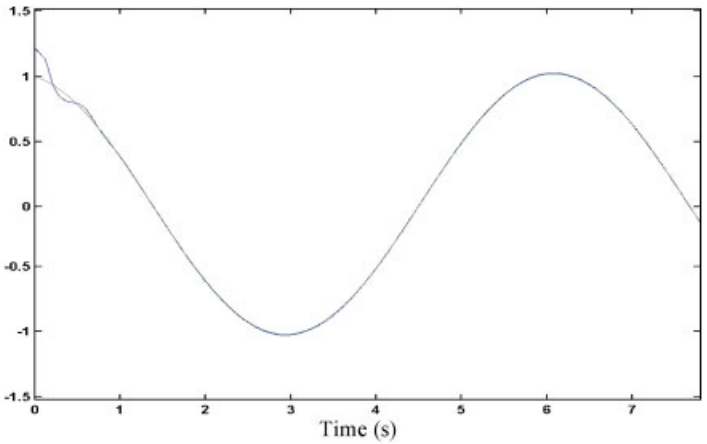

Figure 5. Derivative of signal in the presence of a noise: robust differentiator.

results from a compromise between the noise level and the phase delay between the output of the differentiator and the ideal derivative. In the case of pneumatic systems, a comparative study between some differentiation algorithms in real time was carried out. Among these algorithms that which offers the best compromise between the level of noise on the derived signal and the phase delay is given by the following equation [32]:

$$\dot{x}_n = \frac{x_n - x_{n-2}}{2T_s} \tag{41}$$

In order to compare the differentiation algorithm (41) with (34), a sinusoidal signal with noise was applied as an input. The output of the two differentiators, as well as the analytical derivative, are reproduced in Figures 5 and 6. In Figure 5, one notices that (34) converges towards the analytical derivative in a finite time. The differentiator is insensitive to high-frequency components of the input signal while the output of the differentiation algorithm (41) consists of the accurate derivative and some high-frequency noise (see Figure 6). The use of this last in the context of controlling electropneumatic system (for example, to calculate acceleration from velocity) introduced inevitably the chattering phenomena.

As indicated previously, the choice of a differentiator results from a compromise between the noise level and phase delay. The relative importance of these two criteria depends on the experimental context; it is difficult to show the superiority of a differentiation algorithm in the absence of experimental data. For that, we try thereafter to compare the two differentiators and their influences on the control of an electropneumatic system.

6. EXPERIMENTAL RESULTS

These controllers (15) and (28) were implemented using a dSpace DS1104 controller board with a dedicated digital signal processor. The sensed signals, all analog, were run through the signal conditioning unit before being read by a 16 bits A/D converter.

DOI: 10.1002/rnc

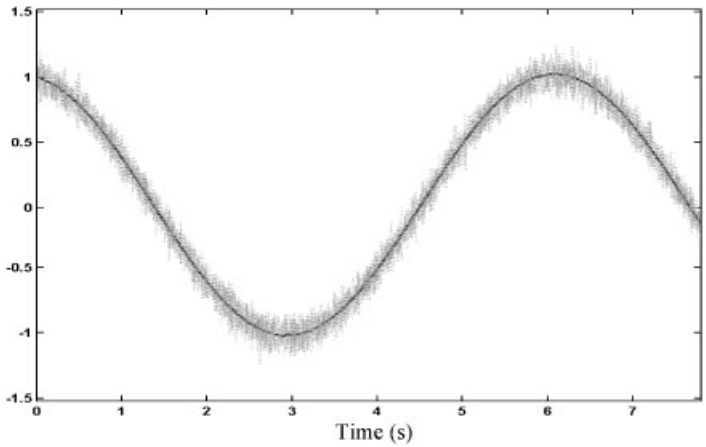

Figure 6. Derivative of signal in the presence of a noise: classical differentiator.

There are two ways to obtain velocity feedback, namely, using a sensor to measure velocity or using position information to generate velocity signals. To reduce the cost of the system, the velocity of the cylinder is determined by analogically differentiating and low-pass filtering the position. The control law is therefore implemented using three sensors: a position sensor and two pressure sensors.

The position sensor is a NovoTECHNIK, model TLH500. Its linearity error is $\pm 0.05\%$. The two pressure sensors are made by KULITE model XT140M-7BarA, their precision is equal to 700 Pa (0.1%) and their combined nonlinearity and hysteresis errors is $\pm 0.1\%$.

6.1. Second-order sliding mode controller results

The aim of the control law is to keep a good accuracy in terms of position tracking for the desired trajectory (see Figure 2) in spite of model uncertainties and load variation.

Firstly, the total load mass equals 17 kg (nominal case). The proposed algorithm (15) is applied and (41) is used to recover the acceleration information. The controller parameters λ and α_2 have been tuned to satisfy condition (10). The test has been made several times in order to evaluate the repeatability of the experimental results. Figures 7–9 show the position error, the estimated acceleration and the desired acceleration, and the control input.

The maximum position error is about 1.5 mm, 0.6% of the total displacement magnitude (see Figure 7). In [4], a hybrid of fuzzy and PID control algorithm is proposed for point-to-point displacement. In this case, the steady-state error is about 3.5 mm (the total displacement is equal to 200 mm). A PID controller augmented with friction compensation using neural network is presented in [33]. A sinusoid with magnitude of 70 mm and frequency of 0.2 Hz has been used as reference input. In this case, the maximum position error is about 8.1 mm. From this point of view, the obtained results with the second-order sliding mode controller are therefore more attractive. However, by the effect of acceleration signal, the control input is affected by the chattering phenomena generating a significant noise level. In [12], the author relates the chattering behaviour to the discontinuity of the 'sign' function which appears in the control law

DOI: 10.1002/rnc

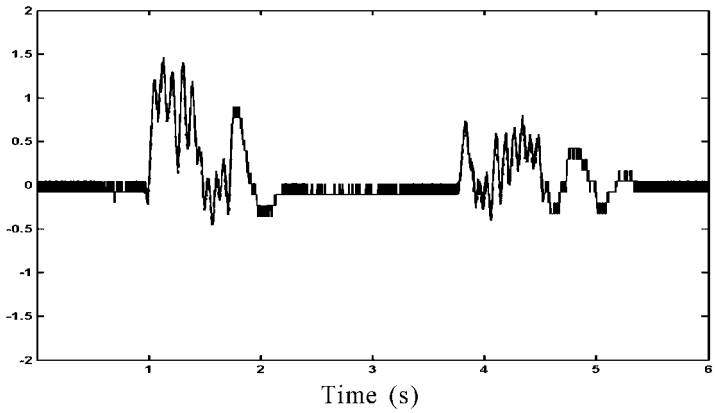

Figure 7. Nominal mass = 17 kg. Position error (mm) *versus* time.

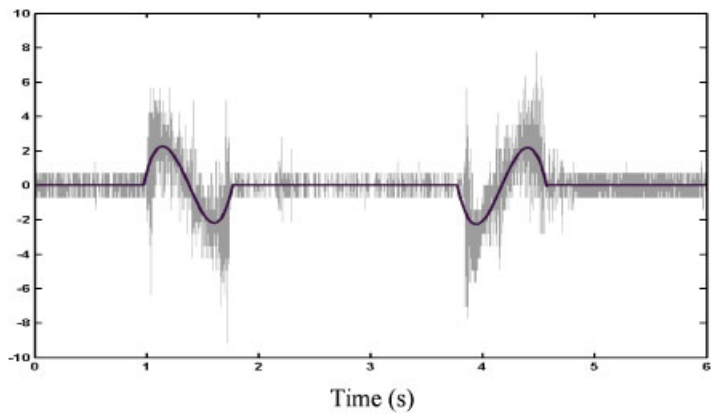

Figure 8. Acceleration and desired acceleration ($m\,s^{-2}$) *versus* time.

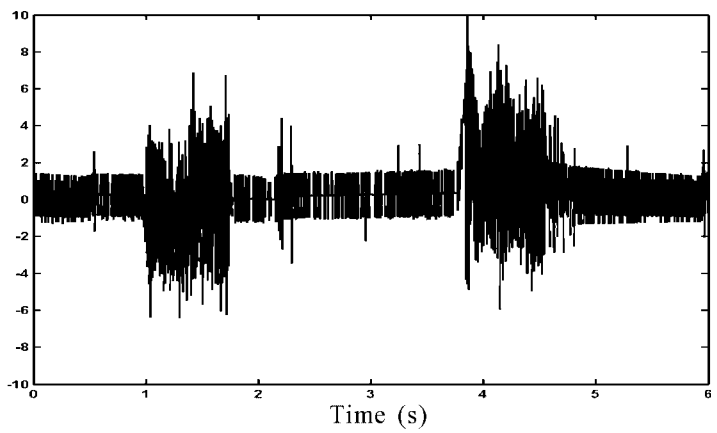

Figure 9. Control input (V) *versus* time.

DOI: 10.1002/rnc

on the sliding manifold. To overcome this problem, one can replace the 'sign' function in a small vicinity of the surface by a smooth approximation, the so-called boundary layer control that implies deterioration of accuracy and robustness. Note that this solution is not enough in pneumatic field [9] indeed, a good compromise between static position error and chattering cannot be found.

In order to ensure a better derivation of velocity in real time, (34) is used to recover the acceleration signal. Some experimental results are provided here to demonstrate the effectiveness of the combined (15)–(34). Figure 11 shows the estimated acceleration and the desired acceleration. It is important to note that, although the velocity signal is obtained by analog differentiation of the position (in other words, the velocity signal contains some small high-frequency noise), the acceleration signal is smooth. Moreover, the resulting acceleration is without harmful delay. This improves the effectiveness of (15).

Indeed, the maximum position error is about 0.79 mm (see Figure 10), i.e. twice smaller than the maximum position error obtained with the same controller combined with (41).

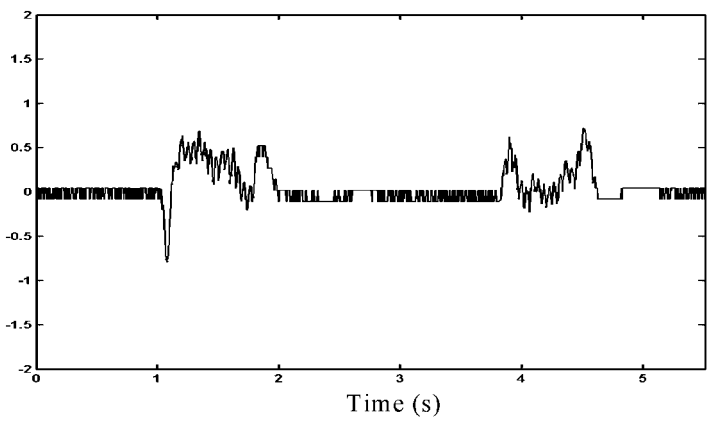

Figure 10. Nominal mass = 17 kg. Position error (mm) *versus* time.

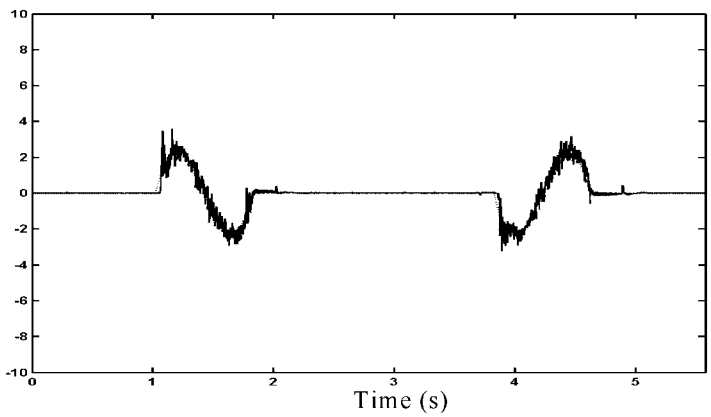

Figure 11. Acceleration and desired acceleration ($m\,s^{-2}$) *versus* time.

DOI: 10.1002/rnc

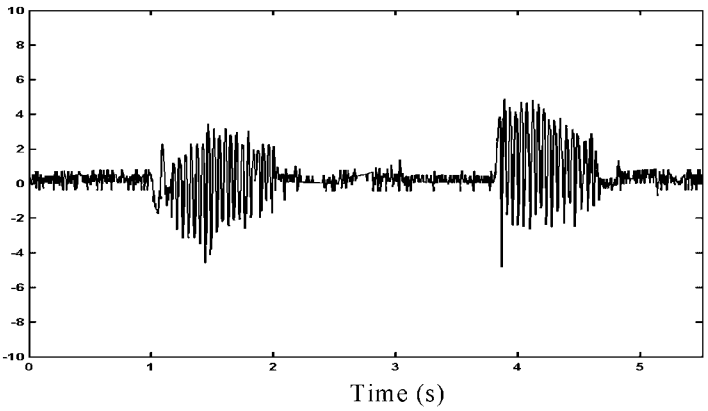

Figure 12. Control input (V) *versus* time.

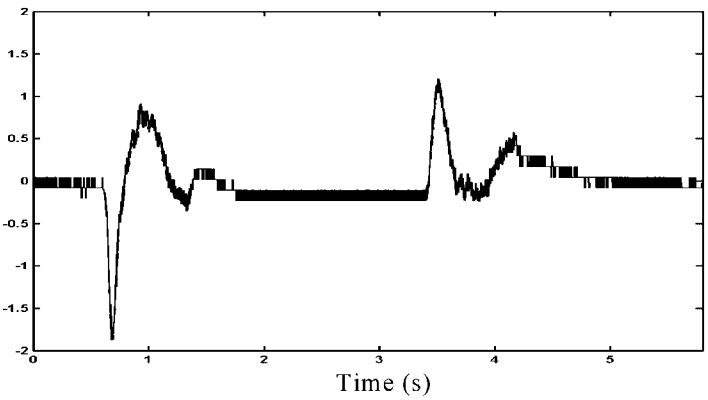

Figure 13. Modified mass = 32 kg. Position error (mm) *versus* time.

Figure 12 displays the control input. The chattering phenomena are significantly reduced but are not completely eliminated. The actuators and sensors parasitic dynamics are the main cause of the chattering effect as well described in several papers [34, 35]. However, the magnitude of the oscillations could be considered as acceptable. Even if the signal excites the spool valve during the static and dynamic stages, no audible noise can be heard contrary to first-order sliding mode control [15].

In order to illustrate the robustness of the proposed differentiator–controller design, the total load mass is increased until 32 kg. The presented results are obtained without changing the control gain value. The design robustness against the load mass variation can be observed in Figure 13. The maximum position tracking error is about 1.9 mm. In steady state, the position error is about 140 μm.

6.2. Third-order sliding mode controller results

Equation (28) is used to track the desired position. As mentioned previously, firstly (41) is used to recover the acceleration information. Figures 14–16 show the position error, the estimated acceleration and the desired acceleration, and the control input, respectively.

DOI: 10.1002/rnc

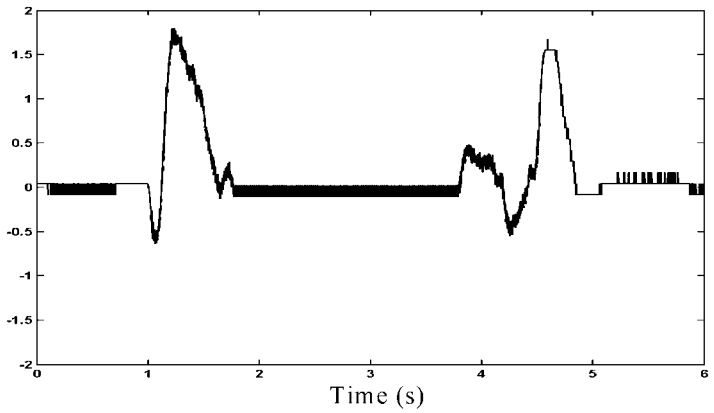

Figure 14. Nominal mass = 17 kg. Position error (mm) *versus* time.

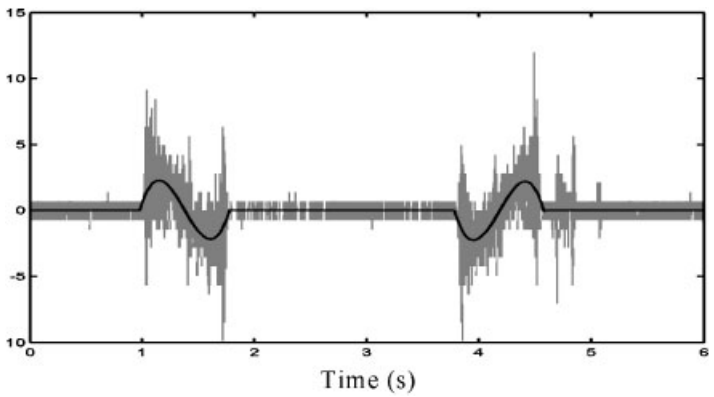

Figure 15. Acceleration and desired acceleration ($m\,s^{-2}$) *versus* time.

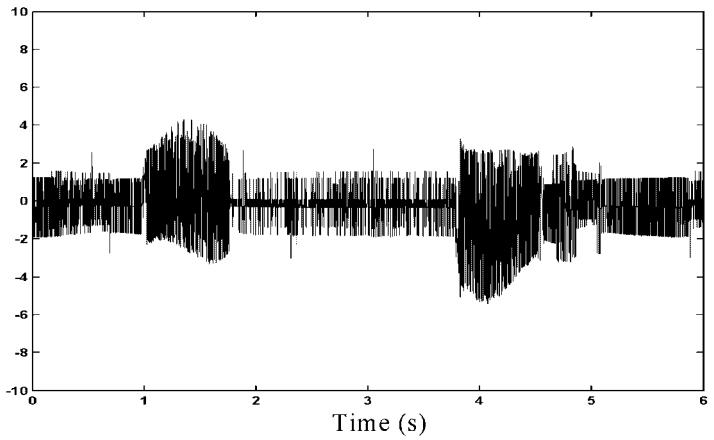

Figure 16. Control input (V) *versus* time.

DOI: 10.1002/rnc

In this case, the maximum position error is about 1.8 mm. In [2], a classical linear control law with scheduling gains, based on the local linearization of the nonlinear dynamics about a nominal operating point is proposed. The control law has been implemented on the same experimental plant and under same conditions. By using the same desired position (i.e. the maximum desired velocity is equal to 0.6 m/s), this control algorithm [2] is applied to the electropneumatic system. The maximum position error is in this case about 4.26 mm. So the better performances are obtained using HOSM controller in terms of position tracking. However, the control input is affected by the chattering effect.

In order to reduce the chattering phenomena, (34) is used to recover the acceleration. Figures 17–19 show the position error, the estimated acceleration and the desired acceleration, and the

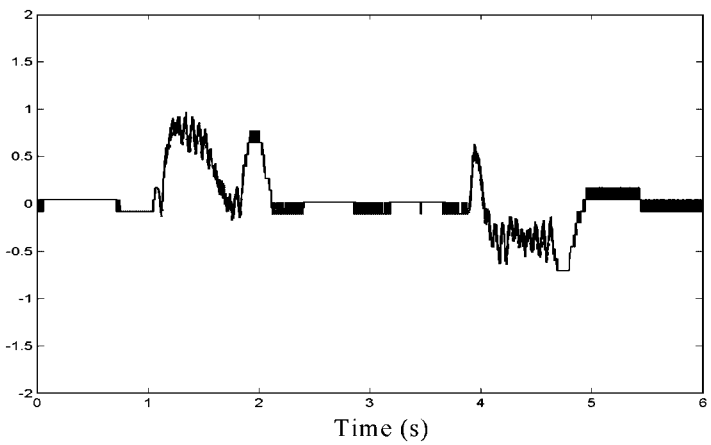

Figure 17. Nominal mass = 17 kg. Position error (mm) *versus* time.

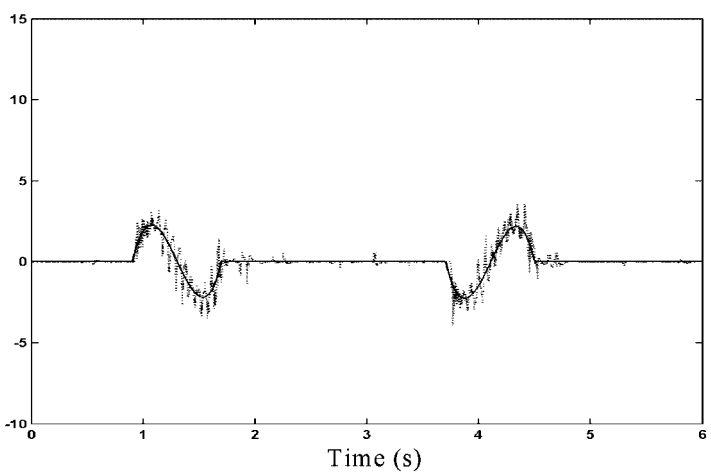

Figure 18. Acceleration and desired acceleration ($m\,s^{-2}$) *versus* time.

DOI: 10.1002/rnc

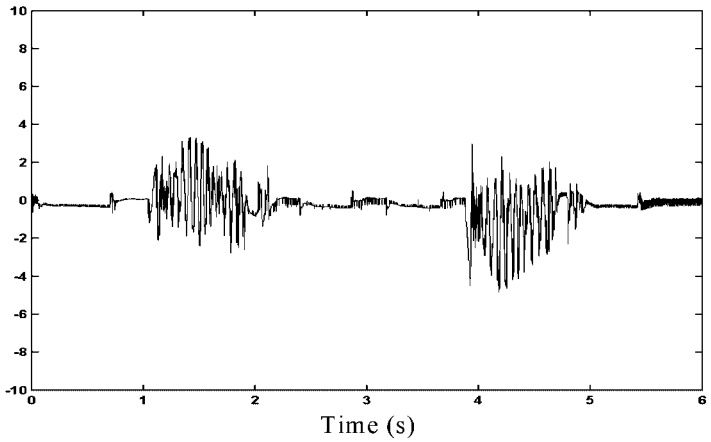

Figure 19. Control input (V) *versus* time.

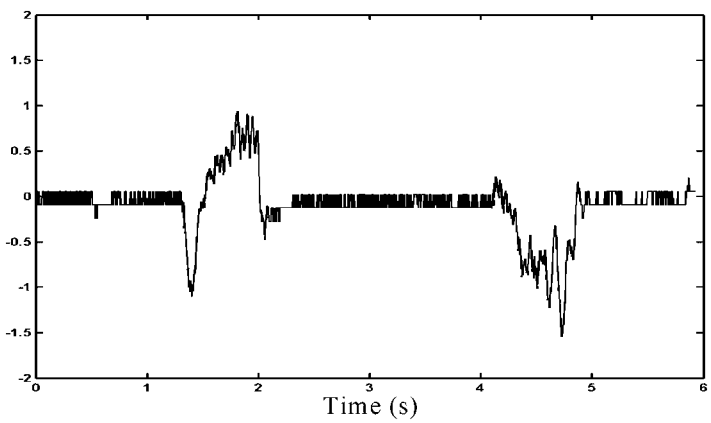

Figure 20. Modified mass = 32 kg. Position error (mm) *versus* time.

control input, respectively. The experimental results show that the undesired chattering effect is reduced and a good tracking position is obtained: the maximum position error is less than 1 mm. In steady state, the position error is about 110 μm. From these experimental results, we can conclude that the use of (34) makes it possible to ensure a better derivation of velocity in real time and thus to ensure a good accuracy in terms of position tracking for a desired trajectory. However, it is important to note that the position error is also the sliding variable. It is apparent that whenever the position changes, the sliding variable is not zero.[§] The presence of the actuators and sensor parasitic dynamics [36] introduces a resonant mode which can be excited by fast variations.

[§]The same remark can be done with respect to the experiment results using the 2-sliding controller.

DOI: 10.1002/rnc

Finally, in order to illustrate the robustness of the combined (28) and (34), the total load mass M is increased to 32 kg. The presented results are obtained without changing the control gain value. The maximum position tracking error is about 1.55 mm (Figure 20). In steady state, the position error is about 110 μm.

For comparison purpose, a classical linear control law with scheduling gains [2] has been implemented on the same experimental plant ($M = 32$ kg), in the same conditions. In this case, the maximum position error is about 7.8 mm. Our proposed approach is demonstrated to be steady-state performances, robustness against parameter uncertainties, and perturbation the main features of the proposed method.

7. CONCLUSION

In this paper, a combined robust differentiator and robust controllers *via* HOSM for an electropneumatic system have been presented. It is well known that the performance of this combination depends on the experimental context. For this, experimental results are carried out in order to show the effectiveness of this structure.

The difficulties traditionally associated with the use of estimated acceleration variable for state-feedback controller of electropneumatic system have been studied. The differentiator unit has been used to estimate the acceleration. The method shows remarkable results. The proposed algorithm efficiently attenuates the noise related to differentiating the velocity signal while maintaining the delay differentiation properties. This improvement permits jointly to reduce the noise in control signal and hence the reduction of chattering effect, and to increase the tracking performance in terms of tracking position error. Moreover, the energy consumption decreases while at the same time the lifetime of the components is extended. Presently, the implementation of double numerical differentiator in order to obtain velocity and acceleration signals is under study. The proposed design can be applied in other industrial environments with mechanical, hydraulic, and electrical components.

APPENDIX: NOMENCLATURE

b	viscous friction coefficient (N/m/s)
k	polytropic constant
M	total load mass (kg)
p	pressure in the cylinder chamber (Pa)
q_m	mass flow rate provided from servodistributor to cylinder chamber (kg/s)
r	perfect gas constant related to unit mass (J/kg/K)
S	area of the piston cylinder (m^2)
T	temperature (K)
V	volume (m^3)
y, v, a, j	position (m), velocity (m/s), acceleration (m/s^2), jerk (m/s^3)
$\varphi(.)$	leakage polynomial function (kg/s)
$\psi(.)$	polynomial function (kg/s/V)
l	length of stroke (m)
T_s	sample time

DOI: 10.1002/rnc

s	sliding surface
u	control input

Subscript

ext	external
D	dead volume
S	supply
N	chamber N
P	chamber P
d	desired

REFERENCES

1. Edge KA. The control of fluid power systems responding to the challenge. *Journal of Systems and Control Engineering* 1997; **211**(12):91–110.
2. Brun X, Sesmat S, Thomasset D, Scavarda S. A comparative study between two control laws of an electropneumatic actuator. *European Control Conference ECC'99*, CD Rom, Karlsruhe, 1999; 6, reference F1000-5.
3. Kimura T, Hara S, Fujita T, Kagawa T. Feedback linearization for pneumatic actuator systems with static fiction. *Control Engineering Practice* 1987; **5**(10):1385–1394.
4. Parnichkun M, Ngaecharoenkul C. Kinematics control of a pneumatic system by hybrid fuzzy PID. *Mechatronics* 2001; **11**:1001–1023.
5. Li B, Li Z, Xu Y. Study on adaptive control for a pneumatic position servo system. *Advances in Modelling and Analysis* 1997; **49**(2):21–28.
6. Smaoui M, Brun X, Thomasset D. A study on tracking position control of an electropneumatic system using backstepping design. *Control Engineering Practice* 2006; **14**(8):923–933.
7. Mattei M. Robust regulation of the air distribution into an arc heater. *Journal of Process Control* 2001; **11**:285–297.
8. Utkin VI. Variable structure systems with sliding modes. *IEEE Transactions on Automatic Control* 1977; **26**(2): 212–222.
9. Bouri M, Thomasset D. Sliding control of an electropneumatic actuator using an integral switching surface. *IEEE Transactions on Control Systems Technology* 2001; **9**(2):368–375.
10. Smaoui M, Brun X, Thomasset D. Systematic control of an electropneumatic system: integrator backstepping and sliding mode control. *IEEE Transactions on Control Systems Technology* 2006; **14**(5):905–913.
11. Song J, Ishida Y. A robust sliding mode control for pneumatic servo systems. *International Journal of Engineering Science* 1997; **35**(8):711–723.
12. Slotine JE, Li W. *Applied Nonlinear Control*. Prentice-Hall: Englewood Cliffs, NJ, 1991; 461.
13. Levant A. Sliding order and sliding accuracy in sliding mode control. *International Journal of Control* 1993; **58**(6):1247–1263.
14. Laghrouche S, Smaoui M, Brun X, Plestan F. Robust second order sliding mode controller for electropneumatic actuator. *American Control Conference*, *ACC*, Boston, U.S.A., 2004; 5090–5095.
15. Laghrouche S, Smaoui M, Plestan F, Brun X. Higher order sliding mode control based on optimal approach of an electropneumatic actuator. *International Journal of Control* 2006; **79**(2):119–131.
16. Gauthier JP, Hammouri H, Othman S. A simple observer for nonlinear systems applications to bioreactors. *IEEE Transactions on Automatic Control* 1992; **37**(6):875–880.
17. Krener AJ, Kang W. Locally convergent nonlinear observers. *SIAM Journal on Control Optimization* 2003; **42**(1):155–177.
18. Ibrir S. Linear time-derivative trackers. *Automatica* 2004; **40**:397–405.
19. Valiviita S, Ovaska SJ. Delayless recursive differentiator with efficient noise attenuation for control instrumentation. *Signal Processing* 1998; **69**:267–280.
20. Levant A. Robust exact differentiation via sliding mode technique. *Automatica* 1998; **34**(3):379–384.
21. Shearer JL. Study of pneumatic processes in the continuous control of motion with compressed air, Parts I and II. *Transactions on American Society for Mechanical Engineering* 1956; **78**:233–249.
22. Araki K. Effects of valve configuration on a pneumatic servo. *International Fluid Power Symposium*, Cambridge, 1981; 271–290.

DOI: 10.1002/rnc

23. Richard E, Scavarda S. Comparison between linear and nonlinear control of an electropneumatic servodrive. *Journal of Dynamic Systems, Measurement, and Control* 1996; **118**:245–252.
24. Sesmat S, Scavarda S. Static characteristics of a three way servovalve. *Twelfth Aachen Conference on Fluid Power Technology*, Aachen, Germany, 1996; 643–652.
25. Belgharbi M, Thomasset D, Scavarda S, Sesmat S. Analytical model of the flow stage of a pneumatic servodistributor for simulation and nonlinear control. *Sixth Scandinavian International Conference on Fluid Power, SICFP'99*, Tampere, Finland, 1996; 847–860.
26. Brun X, Thomasset D, Bideaux E. Influence of the process design on the control strategy: application in electropneumatic field. *Control Engineering Practice* 2002; **10**(7):727–735.
27. Bartolini G, Ferrara A, Usai E. Chattering avoidance by second-order sliding mode control. *IEEE Transactions on Automatic Control* 1998; **43**(2):241–246.
28. Fridman L, Levant A. Higher order sliding modes. *Sliding Mode Control in Engineering*. Marcel Dekker: New York, 2002; 53–101.
29. Brun X, Belgharbi M, Sesmat S, Thomasset D, Scavarda S. Control of an electropneumatic actuator, comparison between some linear and nonlinear control laws. *Journal of Systems and Control Engineering* 1999; **213**(I5):387–406.
30. Levant A. Universal SISO sliding-mode controllers with finite-time convergence. *IEEE Transactions on Automatic Control* 2001; **46**(9):2001; 1447–1451.
31. Levant A. Higher-order sliding modes, differentiation and output-feedback control. *International Journal of Control* 2003; **76**(9):924–941.
32. Richard E. De la commande linéaire et non linéaire en position des systèmes électropneumatiques. *Ph.D. Thesis*, INSA de Lyon, 1990; 291 (in French).
33. Lee HK, Choi GS, Choi GH. A study on tracking position control of pneumatic actuators. *Mechatronics* 2002; **12**:813–831.
34. Fridman LM. An averaging approach to chattering. *IEEE Transactions on Automatic Control* 2001; **46**(8): 1260–1265.
35. Boiko I, Fridman L, Castellanos MI. Analysis of second-order sliding-mode algorithms in the frequency domain. *IEEE Transactions on Automatic Control* 2004; **49**(6):946–950.
36. Allotta B, Pisano A, Pugi L, Usai E. VSC of a servo-actuated ATR90-type pantograph. *Proceedings of the 44th IEEE Conference on Decision and Control* (*CDC'05*), Sevilla, Spain, December 2005; 590–595.

DOI: 10.1002/rnc